Pergamon

Scripta Metallurgica *et* Materialia, Vol. 33, No. 12, pp. 1999-2005, 1995
Elsevier Science Ltd

0956-716X/95 $9.50 + .00

0956-716X(95)00475-0

THE EFFECT OF Nb-ADDITION ON THE $L1_2$ PRECIPITATES OF RAPIDLY-SOLIDIFIED Al-Cr-Zr ALLOY

M.S. Chuang and G.C. Tu
Institute of Materials Science and Engineering, National Chiao Tung University, Hsinchu, Taiwan, R.O.C

(Received May 15, 1995)
(Revised July 18, 1995)

Introduction

Development of dispersion strengthened aluminum alloys for elevated temperature application is an active field of research in the past decade [1-8]. For high temperature Al alloys, the dispersed strengthening phase must not undergo an undesirable phase transformation during long time exposure at the temperature of interest. An additional factor to be considered is the stability of the strengthening phase with respect to Ostwald ripening. In Ostwald ripening, larger particles grow at the expense of smaller ones driven by reduction of the total interfacial free energy. According to theory, a particle will be resistant to coarsening if the diffusivity D and solubility C_0 of its rate-controlling element is small, and if the energy of its interface with the matrix, σ, is low.

Aluminum alloys containing $L1_2$-Al_3Zr dispersed phase are good candidates for high temperature usage. Among the transition elements, Zr has the lowest diffusivity flux DC_0 in Al [9]. Furthermore, the $L1_2$-Al_3Zr phase is coherent and coplanar with the Al matrix, the lattice misfit, and thus the interfacial energy is small. These meet the requirements for a low Ostwald ripening rate. However, it was suggested that careful selection of additional alloying elements could further reduce the misfit, thereby reducing σ and ripening rate of the $L1_2$ phase [10].

Henry et al. [11] had calculated the lattice parameter and the disregistry to pure aluminum for a number of $L1_2$-Al_3M. $L1_2$-Al_3Ti phase is calculated to be with the smallest degree of lattice disregistry, and only the $L1_2$-Al_3V phase has a negative lattice mismatch. On the other hand, the lattice disregistry between $L1_2$-Al_3Zr and pure Al is relatively large. Assuming Vegard's law holds for a combination of $L1_2$-Al_3Zr with $L1_2$-Al_3Ti and/or $L1_2$-Al_3V, it would be possible to form co-intermetallic $L1_2$-$Al_3(Zr,M)$ compounds which match Al matrix better than $L1_2$-Al_3Zr does. In fact, it was reported that the interfacial energy σ of $L1_2$ phase in Zr-containing Al alloys can be reduced by additions of V [1–3] or Ti [6–7] to form $L1_2$-structured co-intermetallics $Al_3(Zr,V)$ and $Al_3(Zr,Ti)$.

Disregistry between $L1_2$-Al_3Nb and Al matrix calculated by Henry et al. [11] has a positive value larger than that of $L1_2$-Al_3Ti but lower than that of $L1_2$-Al_3Zr. However, the lattice parameter of $L1_2$-Al_3Nb had been proposed to be 0.3991 [12] and 0.3753 nm [13], this would predict negative values of disregistry, -1.45% and -7.33%, between $L1_2$-Al_3Nb and Al matrix. If the lattice disregistry between $L1_2$-Al_3Nb and Al matrix is negative, as with $L1_2$-Al_3V, addition of Nb to the Zr-containing Al alloys will significantly reduce the lattice disregistry and the interfacial energy of the $L1_2$ phase. Furthermore, according to phase diagram, the Nb-

containing phases are not expected to form at grain boundaries as readily as $Al_{10}V$ does such that formation of $L1_2$ phase precipitate free zones (PFZs) [3] can be avoided.

In the present work, Nb was added to a rapidly solidified Al-Cr-Zr alloy. The age-hardenable Al-Cr-Zr alloys derive their elevated strength from homogeneous precipitation of $L1_2$-Al_3Zr and chromium retained in solid solution [4–5]. The effect of Nb addition on the $L1_2$ phase was studied in terms of its coarsening kinetics, interfacial energy, and particle size distribution.

Experimental Procedure

A rapidly solidified Al-Cr-Zr-Nb ribbon prepared by melt-spinning was under examination in the present work. The typical composition determined by inductively coupled plasma-mass spectrometer (ICP) was: Al-3.14Cr-4.03Zr-1.95Nb (in wt%). This composition was designed to precipitate about 8 vol% of $L1_2$-$Al_3(Zr_{0.67}Nb_{0.33})$ particles. A prealloyed ingot was induction-melted in a graphite crucible in Ar atmosphere using commercially pure Al(99.9%), Cr(99.8%), Zr(99.9%), and Nb(99.9%). Rapidly quenched ribbons about 30 μm thick and 5 mm width, were prepared from the prealloyed ingots under He atmosphere using a single roller melt-spinning apparatus with a copper roller rotating at a surface velocity about 33 m/s.

The microstructures of the as-spun ribbons shows no obvious precipitate on the chilled side and middle region of the ribbon, indicating that the solutes were in metastable solid solution in the aluminum matrix. However, precipitates about 0.2 μm exist in the region very near to the air side of the ribbon. The specimens investigated in this study were chosen by grounding both side of specimens on a silicon carbide paper to reveal the microstructure of the middle region of the ribbon. To precipitate the L12 phase, all samples used in this study were aged at 450°C for 1 hr. Some of the aged samples were then annealed at 375 or 400°C for 100, 240, 500, and 1000 hrs. A few aged samples were further annealed at 450°C for up to 100 hrs. Thin foils for scanning transmission electron microscope (STEM) observation were prepared in a double-jet polishing apparatus in a standard solution. The STEM used was JOEL JEM-2000FX, operating at 200 kV. The $L1_2$ particle sizes were measured directly from TEM negatives which were taken by the central dark field technique from superlattice reflection spots. An eyepiece magnifier with a calibrated scale was used as an aid. More than 1000 particles were measured to obtain each value of mean radius, $\bar{r}$.

Results and Discussion

Figure 1 is a TEM dark field (DF) micrograph of ribbons aged at 450°C for 1 hr using a diffracted spot of the $L1_2$ structured precipitates. The inserted TEM selected area diffraction pattern (SADP) of the precipitates is consistent with the $L1_2$ structure. A cube/cube orientation relationship with Al matrix exist for this $L1_2$ phase. It is apparently shown in Fig. 1 that copious L12 particles precipitate homogeneously throughout the whole matrix in aging. The mean particle radius of the precipitates is 1.0 nm. Theoretically, the fine particle size and the homogeneous distribution of $L1_2$ particles in bulk matrix would result in a good precipitation hardening property to the alloy. Indeed, Vickers hardness tests show that the microhardness rises from 113 kg/mm^2 of as-spun ribbon to 204 kg/mm^2 of as-aged ribbon.

A coarsening study of the spherical $L1_2$ particles was carried out at 375, 400, and 450°C in ribbons aged at 450°C for 1 hr. Figs. 2a-2f show $L1_2$ particles in aged ribbons after being annealed at 375, 400, and 450°C for various times. The increase in mean particle radius, $\bar{r}$, with increase in annealing temperature and time is seen although not so apparently except in the case of 450°C. More than 1000 particles were measured to obtain each value of $\bar{r}$. It is notable that, even for 1000 hrs annealing at 375, and 400°C, the mean particle radius of the spherical L12 particles are still only 2.0 and 3.2 nm, respectively. According to the modified Lifshitz-Slyozov-Wagner (LSW) theory of volume diffusion controlled coarsening [14,15], the mean particle radius should increase in accordance with the relationship

$$\bar{r}^3 - \bar{r}_0^3 = K(t - t_0) \tag{1}$$

where $\bar{r}$ is the mean particle radius at time t, $\bar{r}_0$ is the value corresponding to t_0, and K represents the volumetric coarsening rate constant. If the effect of the precipitate volume fraction on the Ostwald ripening is taken into account, the coarsening rate constant K for an alloy containing 8 vol% precipitates is given by [16]

$$K = \frac{13\,\sigma D C_0 V_m^2}{9\nu RT} \tag{2}$$

where σ is the interfacial energy of the particle, D is the diffusivity of the rate-controlling solute, C_0 is the solubility limit of that component in the matrix, ν is the stoichiometric factor, and V_m is the molar volume of the particle, R and T have their usual meanings. Fig. 3 shows the coarsening kinetics of the $L1_2$ particles at 375, 400, and 450 C, where the values of $(\bar{r}^3 - \bar{r}_0^3)$ are plotted versus annealing time. The linear correlation coefficients of the best fit lines of the three lines are all very near to unit, this suggests that the coarsening kinetics of the $L1_2$-structured $Al_3(Zr_{0.67}Nb_{0.33})$ is an LSW type volume diffusion controlled process. From eq. 1, remarkably slow volumetric coarsening rate of 5.73×10^{-30}, 2.51×10^{-29}, 5.86×10^{-28} m^3/hr for the $L1_2$ particles at 375, 400 and 450°C, respectively, are obtained. These values are comparable to those of $L1_2$-structured $Al_3(Zr,Ti)$[7] and $Al_3(Zr,V)$[3] particles in RS aluminum alloys, and are about 2 orders of magnitude smaller than that of $L1_2$-Al_3Zr particle in an arc melted aluminum alloy[1].

To evaluate the interfacial energy σ, of the $L1_2$-$Al_3(Zr_{0.67}Nb_{0.33})$ particles, eq. (2) was used, and Zr is assumed to be the rate controlling component since Zr has the lowest diffusivity flux, DC_0. The value of σ was calculated both on data taken from 375 and 400°C annealing in the present study to examine the accuracy, and both resulting in a value of 0.013 J/m^2. Values of all the parameters used in the above calculation are listed in Table 1. The obtained interfacial energy is reasonable for a coherent precipitate/matrix interface. For example, values of σ from 0.01 to 0.03 J/m^2 for $\gamma'(Ni_3Al)$ in Ni-base alloys [17–19], and 0.014 J/m^2 for $\delta'(Al_3Li)$ in Al-Li alloy[20] had been reported. The agreement between the calculated σ and the measured

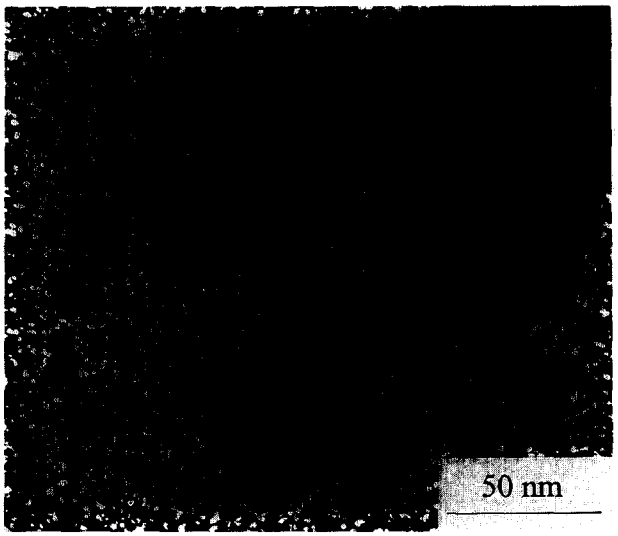

Figure 1. TEM DEF micrograph showing precipitation of $L1_2$-$Al_3(Zr_{0.67}Nb_{0.33})$ particles for specimen aged at 450°C for 1 hr. Foil normal near to $[001]_{Al}$.

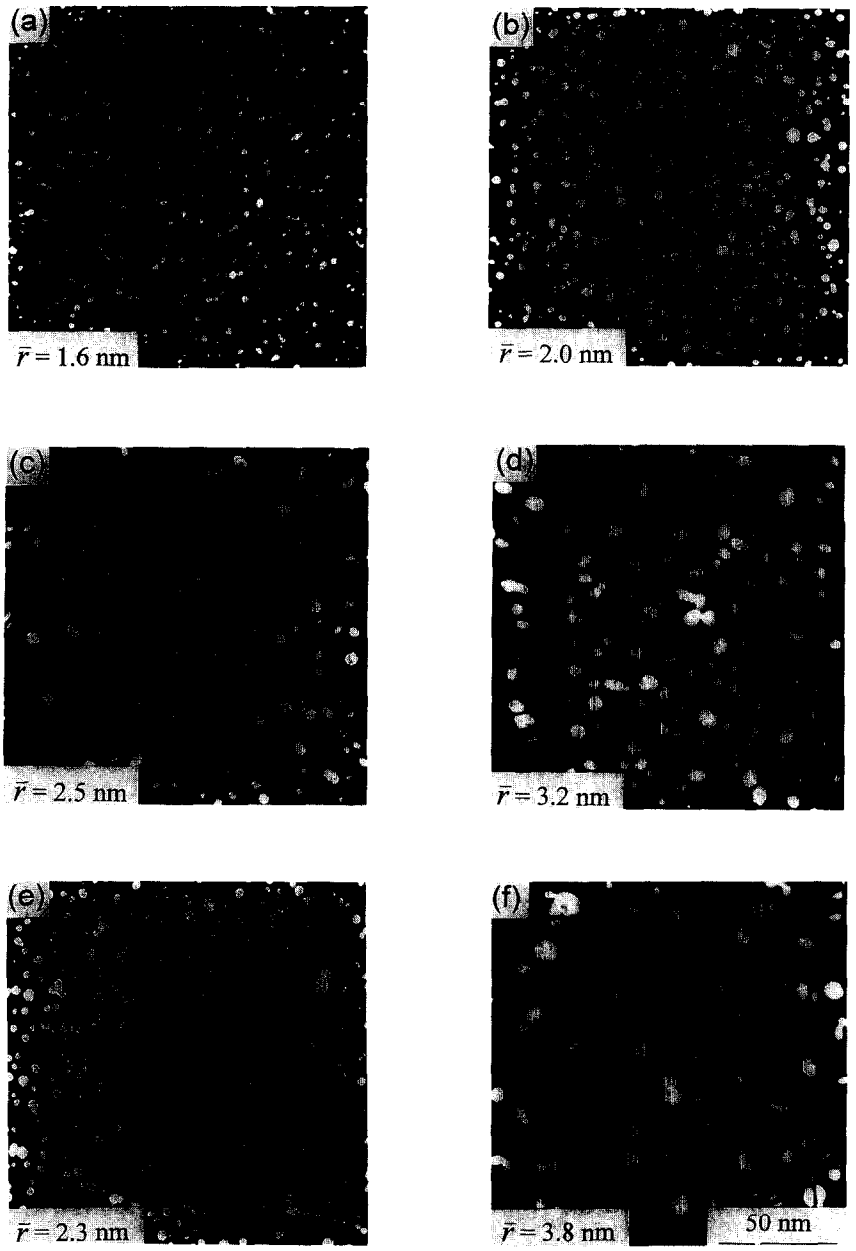

Figure 2. TEM DF micrographs documenting coarsening of $L1_2$-$Al_3(Zr_{0.67}Nb_{0.33})$ precipitates. Specimens were aged at 450 °C for 1 hr then annealing (a) at 375 °C, 500 hrs (b) at 375 °C, 1000 hrs (c) at 400 °C, 500 hrs (d) at 400 °C, 1000 hrs (e) at 450 °C, 24 hrs, and (f) at 450 °C, 100 hrs.

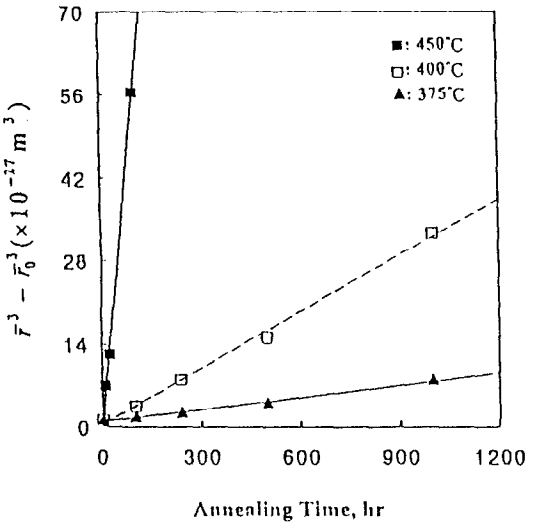

Figure 3. Coarsening kinetics of the $L1_2$-$Al_3(Zr_{0.67}Nb_{0.33})$ precipitates during isothermal annealing at 375, 400, and 450°C. $\bar{r}$ is the mean particle radius at a particular time t. Specimens were preaged at 450°C for 1 hr.

coarsening rates indicates that the coarsening kinetics of the $L1_2$ particles in the present alloy are indeed controlled by volume diffusion of Zr. As compared to the other $L1_2$-structured $Al_3(Zr,M)$ precipitates in RS Al ribbons, $Al_3(Zr_{0.67}Nb_{0.33})$ phase possesses a remarkably low interfacial energy, 0.013 J/m^2. By similar calculation, values of 0.03 J/m^2 for $Al_3(Zr_{0.25}V_{0.75})$ [2] and 0.036 J/m^2 for $Al_3(Zr_{0.6}Ti_{0.4})$ [7], had been reported. This may imply that the disregistry between $L1_2$-Al_3Nb and Al matrix is a negative value.

In addition to deriving the rate of mean particle size change, the LSW theory also predicts the particle size distribution (PSD) of precipitates in dilute alloys systems [14–15]. However, the PSD predicted by LSW theory is only valid in alloys with very small volume fractions of particles. Recently, several modifications of the LSW theory, which take the particle volume fraction effect into account, have been developed [16–19,22]. Ardell [22] presented a modified LSW (MLSW) theory based on the supposition that the solute diffusion is depend on a characteristic distance between particles. The PSDs of the precipitates under investigation show agreement with that predicted by MLSW theory rather than that by LSW theory. Some particle size distributions (PSDs) for the L12-Al3(Zr0.67Nb0.33) precipitates at each temperature investigated are given in Fig. 4. At least 1000 particles were measured for each distribution curve. In Fig. 4, the horizontal axis, ρ ($\rho = r/\bar{r}$), is defined as the effective radius divided by the mean particle radius. The vertical axis, $f(\rho)$, is the

TABLE 1
Values of the Material Parameters Necessary to Determine the Interfacial Energy

T (°C)	K (m^3/hr)	D (m^2/sec)	C_0 (moles Zr/m^3)	V_m (m^3/mole)	ν	Calculated σ (J/m^2)
375	5.73×10^{-30}	*6.88×10^{-21}	**38.01	**4.127×10^{-5}	**1	0.013
400	2.51×10^{-29}	*3.18×10^{-20}	**39.48	**4.127×10^{-5}	**1	0.013

* Reference [1]
** Reference [21]

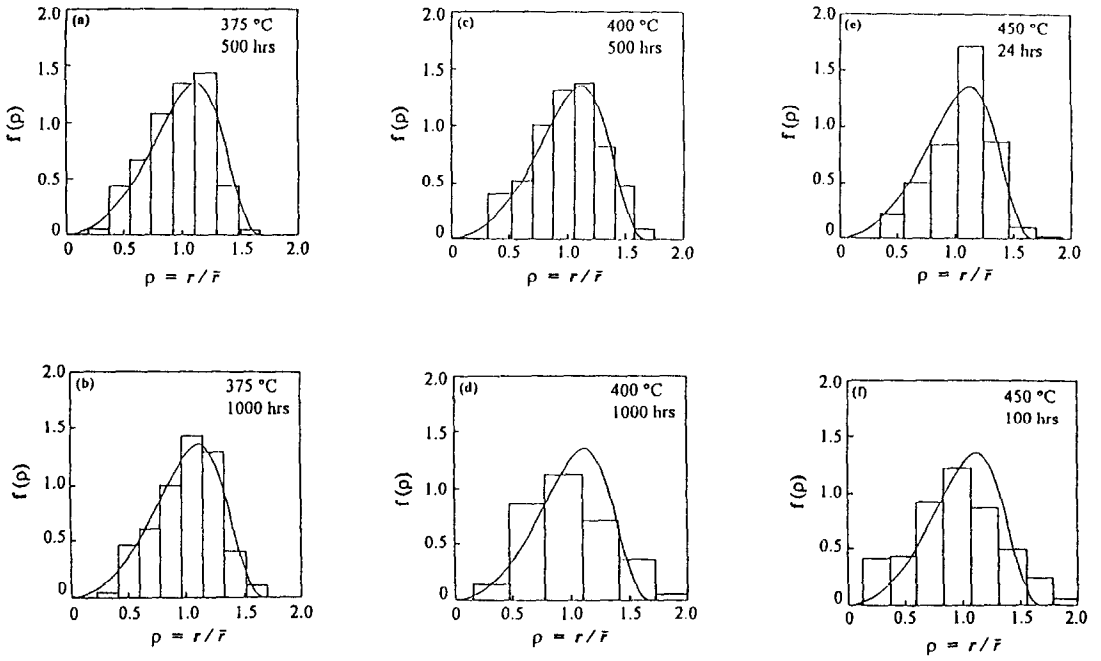

Figure 4. Normalized particle size distributions for Ll_2-$Al_3(Zr_{0.67}Nb_{0.33})$ precipitates annealing at 375, 400, and 450 °C for various times. The superimposed curve shows the predicted MLSW distribution. Specimens were preaged at 450 °C for 1 hr then annealed (a) at 375 °C, 500 hrs, (b) at 375 °C, 1000 hrs, (c) at 400 °C, 500 hrs, (d) at 400 °C, 1000 hrs, (e) at 450 °C, 24 hrs, and (f) at 450 °C, 100 hrs.

relative frequency of occurrence of a given effective radius normalized such that the necessary condition, $\int_0^\infty f(\rho)d\rho = 1$, is met. The superimposed curve in each figure represent the distribution of particles in alloys containing 5 vol% of precipitates predicted by the MLSW theory. As shown in Fig. 4, most of PSDs of the precipitates in the present work fit the curve predicted by MLSW theory, except those at 450 °C for 100 hrs (Fig. 4f) and at 400 °C for 1000 hrs (Fig. 4d). The two unfitted distributions appear more symmetrical and do not show a rapid drop-off feature in high ρ region predicted by MLSW theory. Peaks of these two PSDs shift to lower values of ρ. Discrepancy between these two PSDs and that predicted by MLSW theory may be due to precipitation of coarser equilibrium phase $Al_{13}Cr_2$ in prolonged annealing at high temperature and/or too high annealing temperature, which might repel Zr atom to the adjacent matrix and promote forming coarser L12-Al3Zr precipitates. Further work is in progress to clarify this point.

Summary

A supersaturated Al alloy with 3.14 wt% of Cr, 4.03 wt% of Zr and 1.95 wt% of Nb, which gives rise to about 8 vol% of metastable $L1_2$-$Al_3(Zr_{0.67}Nb_{0.33})$ precipitates after aging, was prepared by the melt spinning process. Spherical L12-structured precipitates with mean particle radius of 10Å form after aging. Slow volumetric coarsening rates of 5.73×10^{-30} (at 375 °C), 2.51×10^{-29} (at 400 °C), and 5.86×10^{-28} (at 450 °C) m^3/hr are measured for the L12-structured $Al_3(Zr_{0.67}Nb_{0.33})$ precipitates in the melt spun ribbon. From a modified LSW equation for volumetric coarsening, an interfacial energy of 0.013 J/m^2 is calculated. This value agrees well with the reported values for a coherent interface. Most particle size distributions (PSDs) of precipitates under investigation also fit quite well to that predicted by MLSW theory. The above points, therefore, prove that Nb is really a useful candidate for addition into an Al-Cr-Zr high temperature Al alloy.

Acknowledgment

We would like to acknowledge the support of the work by the National Science Council of Taiwan, R.O.C. under contract No. 84-2216-E-009-016. Information and some data provision by Drs. M.S. Zedalis and Y.C. Chen are appreciated. Thanks are also due to Prof. C.T. Kuo of Chiao Tung University for help setting up melt-spinning apparatus.

Reference

1. M.S. Zedalis and M.E. Fine, Metall. Trans. A, **17A**, 2187 (1986).
2. Y.C. Chen, M.E. Fine, J.R. Weertman and R.E. Lewis, Scripta Metall., **21**, 1003 (1987).
3. Y.C. Chen, M.E. Fine and J.R. Weertman, Acta Metall. Mat., **38**, 771 (1990).
4. G.J. Marshall, I.R. Hughes and W.S. Miller, Mat. Sci. Tech., **2**, 394 (1986).
5. K. Ioannidis and T. Sheppard, J. Mat. Sci., **26**, 4795 (1991).
6. V.R. Parameswaran, J.R. Weertman and M.E. Fine, Scripta Metall., **23**, 147 (1989).
7. M.S. Chuang and G.C. Tu, Scripta Metall. et Mat., **31**, 1259 (1994).
8. I.H. Moon, J.H. Lee, K.M. Lee and Y.D. Jim, Scripta Metall. et Mat., **32**, 63 (1995).
9. C.M. Adam, in "Rapidly Solidified Amorphous and Crystalline Alloys", (ed. B.H. Kear, B.C. Giessen and M. Cohen), P.411, North-Holland, Oxford (1982).
10. M.E. Fine, Metall. Trans. A, **6A**, 625 (1975).
11. N.F.M. Henry and K. Lonsdale, International Tables for X-ray Crystallography, **1**, 79 (1952).
12. J.H. Xu and A.J. Freeman, Phys. Rev. B, **40**, 11927 (1989).
13. L.F. Mondolfo, in "Aluminum Alloys : Structure and Properties", p.336, London-Boston, Butterworth, (1976).
14. I.M. Lifshitz and V.V. Slyozov, J. Phys. Chem. Solids, **19**, 35 (1961).
15. C. Wagner, Z. Elektrochem., **65** (1961) 581.
16. P.W. Voorhees and M.E. Glicksman, Metall. Trans. A, **15A**, 1801 (1984).
17. A.J. Ardell and R.B. Nicholson, J. Phys. Chem. Solids, **27**, 1793 (1966).
18. A.J. Ardell, Acta Metall., **16**, 511 (1968).
19. P.K. Rastaog and A.J. Ardell, Acta Metall., **19**, 321 (1971) 321.
20. S.F. Baumann and D.B. Williams, Scripta Metall., **18**, 611 (1984).
21. M.S. Zedalis, Ph.D. thesis, Northwestern University, Evanston, Ill. (1985).
22. A.J. Ardell, Acta Metall., **20**, 61 (1972).